



Learning spatial temporal correspondences of cardiac motion from biomechanics-informed modeling

Xiaoran Zhang¹, Chenyu You², Shawn Ahn¹, Juntang Zhuang¹,
Lawrence Staib^{1,2,3} and James Duncan^{1,2,3}

¹Biomedical Engineering, Yale University ²Electrical Engineering, Yale University
³Radiology & Biomedical Imaging, Yale School of Medicine

MICCAI-STACOM 2022

Content I

1 Introduction

2 Motivation

3 Contribution

4 Method

5 Experiments

6 Results

7 Conclusion

8 References

Introduction

- Displacement vector field (DVF) estimated by medical image registration is crucial to infer the underlying spatial temporal dynamics of anatomical structures.
- Accurate prediction of the displacement vector fields (DVF) across cardiac sequences enables regional myocardial strain estimation, which contributes to the localization of infarcted regions of the myocardium [2].

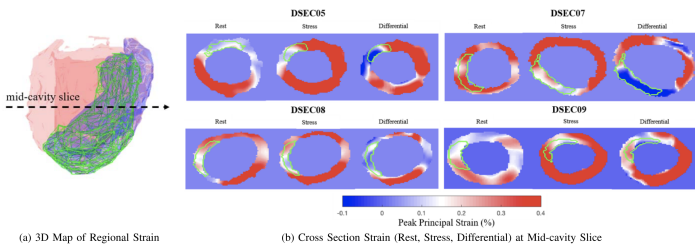


Figure: An example of differential strain map with manually traced myocardial infarct zones (Credit: Lu et al., *IEEE TMI*, 2021 [2]).

Introduction

- Displacement vector field (DVF) estimated by medical image registration is crucial to infer the underlying spatial temporal dynamics of anatomical structures.
- Accurate prediction of the displacement vector fields (DVF) across cardiac sequences enables regional myocardial strain estimation, which contributes to the localization of infarcted regions of the myocardium [2].

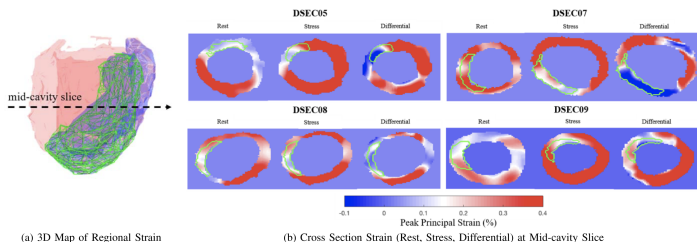


Figure: An example of differential strain map with manually traced myocardial infarct zones (Credit: Lu et al., *IEEE TMI*, 2021 [2]).

Motivation

- **Explicit** biomechanical constraints such as incompressibility often consider biomechanical properties only for specific regions of interest, such as the myocardium.
 - Geometric properties in other structures such as the right ventricle (RV) is not guaranteed.
- To encourage physically plausible transformation, pre-trained variational auto-encoders (VAEs) can be used as regularizers to enforce **implicit** constraints on the DVF.
 - The VAEs are often trained separately on manually generated datasets which require physical simulations.
 - The regularization performance might be limited by VAEs' generalization ability on new datasets.

Motivation

- **Explicit** biomechanical constraints such as incompressibility often consider biomechanical properties only for specific regions of interest, such as the myocardium.
 - Geometric properties in other structures such as the right ventricle (RV) is not guaranteed.
- To encourage physically plausible transformation, pre-trained variational auto-encoders (VAEs) can be used as regularizers to enforce **implicit** constraints on the DVF.
 - The VAEs are often trained separately on manually generated datasets which require physical simulations.
 - The regularization performance might be limited by VAEs' generalization ability on new datasets.

Motivation

- **Explicit** biomechanical constraints such as incompressibility often consider biomechanical properties only for specific regions of interest, such as the myocardium.
 - Geometric properties in other structures such as the right ventricle (RV) is not guaranteed.
- To encourage physically plausible transformation, pre-trained variational auto-encoders (VAEs) can be used as regularizers to enforce **implicit** constraints on the DVF.
 - The VAEs are often trained separately on manually generated datasets which require physical simulations.
 - The regularization performance might be limited by VAEs' generalization ability on new datasets.

Motivation

- **Explicit** biomechanical constraints such as incompressibility often consider biomechanical properties only for specific regions of interest, such as the myocardium.
 - Geometric properties in other structures such as the right ventricle (RV) is not guaranteed.
- To encourage physically plausible transformation, pre-trained variational auto-encoders (VAEs) can be used as regularizers to enforce **implicit** constraints on the DVF.
 - The VAEs are often trained separately on manually generated datasets which require physical simulations.
 - The regularization performance might be limited by VAEs' generalization ability on new datasets.

Contribution

- We propose a biomechanics-informed regularization explicitly as a prior for DVF estimation to preserve geometric properties.
- Our proposed method shows improvement across different cardiac structures due to the more generic assumption.
- We conduct extensive experiments on two public datasets to show its effectiveness and robustness over other competing regularization schemes.

Contribution

- We propose a biomechanics-informed regularization explicitly as a prior for DVF estimation to preserve geometric properties.
- Our proposed method shows improvement across different cardiac structures due to the more generic assumption.
- We conduct extensive experiments on two public datasets to show its effectiveness and robustness over other competing regularization schemes.

Contribution

- We propose a biomechanics-informed regularization explicitly as a prior for DVF estimation to preserve geometric properties.
- Our proposed method shows improvement across different cardiac structures due to the more generic assumption.
- We conduct extensive experiments on two public datasets to show its effectiveness and robustness over other competing regularization schemes.

Method

Framework

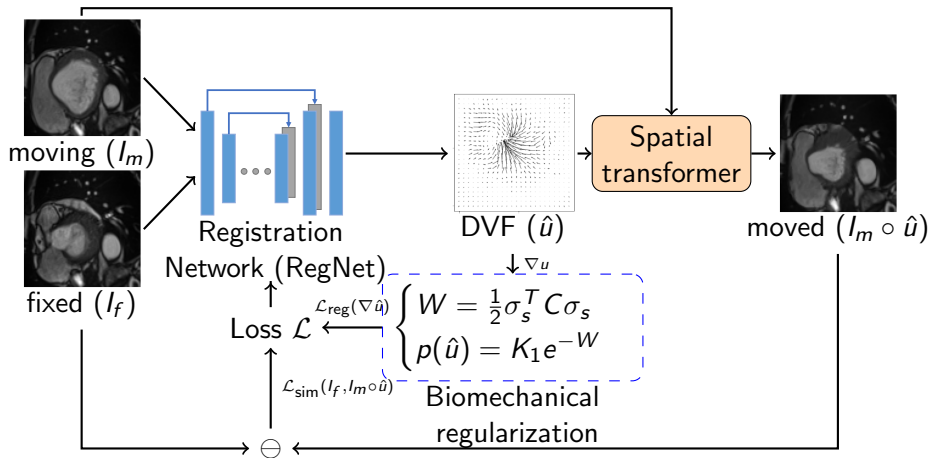


Figure: Illustration of the proposed framework using biomechanics-informed modeling (BIM) for cardiac image registration.

Method

Biomechanics-informed modeling (BIM)

From the classical definition of the strain tensor $\epsilon \in \mathbb{R}^{3 \times H \times W}$ in the infinitesimal linear elasticity model for 2D displacement $\hat{u} = [\hat{u}_1, \hat{u}_2]^T$

$$\epsilon = \left[\frac{\partial \hat{u}_1}{\partial x_1}, \frac{\partial \hat{u}_2}{\partial x_2}, \frac{1}{2} \left(\frac{\partial \hat{u}_1}{\partial x_2} + \frac{\partial \hat{u}_2}{\partial x_1} \right) \right]^T, \quad (1)$$

we define the linear isotropic elastic strain energy density function for each pixel as follows:

$$W_{i,j} = \frac{1}{2} \epsilon_{i,j}^T C \epsilon_{i,j}, \quad (2)$$

where C is the pre-defined stiffness matrix describing material properties of the deforming body

$$C^{-1} = \begin{bmatrix} \frac{1}{E_p} & \frac{-\nu_p}{E_p} & 0 \\ \frac{-\nu_p}{E_p} & \frac{1}{E_p} & 0 \\ 0 & 0 & \frac{2(1+\nu_p)}{E_p} \end{bmatrix}, \quad (3)$$

and E_p is defined as stiffness and ν_p as Poisson ratio.

Methods

Biomechanics-informed modeling (BIM)

The prior probability density function (pdf) of the DVF can be written in Gibb's form:

$$p(\hat{u}) = k_1 e^{-W}. \quad (4)$$

The optimal DVF \hat{u}^* can be obtained through maximum a posteriori (MAP) optimization:

$$\begin{aligned}\hat{u}^* &= \arg \max_{\hat{u}} \left\{ p(\hat{u}|u) = \frac{p(u|\hat{u})p(\hat{u})}{p(u)} \right\} \\ &= \arg \min_{\hat{u}} \left\{ -\log p(u|\hat{u}) - \log p(\hat{u}) \right\}.\end{aligned} \quad (5)$$

Methods

Biomechanics-informed modeling (BIM)

Assume the noise between the measurement u and the DVF estimate \hat{u} is normally distributed $\mathcal{N}(0, \sigma^2)$ [3]

$$p(u|\hat{u}) = \frac{1}{\sqrt{2\pi}\sigma} e^{-\frac{\|u-\hat{u}\|_2^2}{2\sigma^2}}, \quad (6)$$

and from the prior pdf of DVF in Eq. 4, we have our proposed loss.

Proposed biomechanics-informed modeling (BIM) loss

$$\mathcal{L}(I_m, I_f; \hat{u}) = \underbrace{\frac{1}{N} \sum_{i=1}^N \|I_f^i - I_m^i \circ \hat{u}^i\|_2^2}_{\mathcal{L}_{sim}} + \lambda \underbrace{\frac{1}{N} \sum_{i=1}^N \|\epsilon^T C \epsilon\|_2}_{\mathcal{L}_{reg}} \quad (7)$$

Methods

Biomechanics-informed modeling (BIM)

If segmentation labels are given, we have

Proposed biomechanics-informed modeling (BIM) loss

$$\mathcal{L}(I_m, I_f, s_m, s_f; \hat{u}) = \underbrace{\frac{1}{N} \sum_{i=1}^N \|I_f^i - I_m^i \circ \hat{u}^i\|_2^2}_{\mathcal{L}_{sim}} + \lambda \underbrace{\frac{1}{N} \sum_{i=1}^N \|\epsilon^T C \epsilon\|_2}_{\mathcal{L}_{reg}} + \gamma \underbrace{\frac{1}{N} \sum_{i=1}^N \sum_{j=1}^K \left(1 - \text{Dice}\left(s_m^{ij} \circ \hat{u}^i, s_f^{ij}\right)\right)}_{\mathcal{L}_{seg}}, \quad (8)$$

where N is the number of samples and K is the number of cardiac structures.

Dataset details I

ACDC 2017 dataset [1]

- Available at <https://www.creatis.insa-lyon.fr/Challenge/acdc/databases.html>.
- The dataset contains 100 patients including
 - 20 healthy patients
 - 20 patients with previous myocardial infarction
 - 20 patients with dilated cardiomyopathy
 - 20 patients with an hypertrophic cardiomyopathy
 - 20 patients with abnormal right ventricle
- **End-diastolic (ED)** and **end-systolic (ES)** frames are selected from the sequence.
- Segmentation labels consisting of **left ventricle (LV)**, **right ventricle (RV)**, and **epicardium (Epi)** for ED and ES frames are given.
- 60 patients, 20 patients and 20 patients are used for training, validation and testing, respectively.

Dataset details II

LV quantification 2019 dataset [7]

- Available at <https://lvquan19.github.io/>
- The dataset contains 56 subjects and 20 frames are included for the whole cardiac cycle.
- **Endocardium (Endo)** and **epicardium (Epi)** segmentation labels are given for each frame.
- **End-diastolic (ED)** or **end-systolic (ES)** frames are selected from the sequence.
- 34 patients, 11 patients and 11 patients are used for training, validation and testing, respectively.

Experimental setup

- **Experiment design:** ED (moving) to ES (fixed) registration.
- **Preprocessing:** Each slice is cropped to 96×96 with respect to the myocardium centroid after normalization.
- **Implementation:** 1) bspline [6] is implemented using SimpleElastix; 2) optical flow [4] is implemented using scikit-image registration package; 3) learning-based registration is implemented using Pytorch with Adam optimizer with 100 epochs. The learning-based models run 18-30 minutes on a single NVIDIA GTX 2080Ti GPU with 12 GB memory for training and validation.
- **Hyperparameter:** $\nu_p = 0.4$ (Poisson ratio), $\lambda = 0.05$ (weight for BIM loss \mathcal{L}_{reg}), and $\gamma = 0.01$ (weight for auxiliary segmentation loss \mathcal{L}_{seg}).
- **Metrics:** Dice coefficient (DC), Jaccard index (JD), Hausdorff distance (HD), and average symmetric surface distance (ASD) to evaluate segmentation conformance. Jacobian determinant to evaluate the quality of the generated DVF.

Experimental setup

- **Experiment design:** ED (moving) to ES (fixed) registration.
- **Preprocessing:** Each slice is cropped to 96×96 with respect to the myocardium centroid after normalization.
- **Implementation:** 1) bspline [6] is implemented using SimpleElastix; 2) optical flow [4] is implemented using scikit-image registration package; 3) learning-based registration is implemented using Pytorch with Adam optimizer with 100 epochs. The learning-based models run 18-30 minutes on a single NVIDIA GTX 2080Ti GPU with 12 GB memory for training and validation.
- **Hyperparameter:** $\nu_p = 0.4$ (Poisson ratio), $\lambda = 0.05$ (weight for BIM loss \mathcal{L}_{reg}), and $\gamma = 0.01$ (weight for auxiliary segmentation loss \mathcal{L}_{seg}).
- **Metrics:** Dice coefficient (DC), Jaccard index (JD), Hausdorff distance (HD), and average symmetric surface distance (ASD) to evaluate segmentation conformance. Jacobian determinant to evaluate the quality of the generated DVF.

Experimental setup

- **Experiment design:** ED (moving) to ES (fixed) registration.
- **Preprocessing:** Each slice is cropped to 96×96 with respect to the myocardium centroid after normalization.
- **Implementation:** 1) bspline [6] is implemented using SimpleElastix; 2) optical flow [4] is implemented using scikit-image registration package; 3) learning-based registration is implemented using Pytorch with Adam optimizer with 100 epochs. The learning-based models run 18-30 minutes on a single NVIDIA GTX 2080Ti GPU with 12 GB memory for training and validation.
- **Hyperparameter:** $\nu_p = 0.4$ (Poisson ratio), $\lambda = 0.05$ (weight for BIM loss \mathcal{L}_{reg}), and $\gamma = 0.01$ (weight for auxiliary segmentation loss \mathcal{L}_{seg}).
- **Metrics:** Dice coefficient (DC), Jaccard index (JD), Hausdorff distance (HD), and average symmetric surface distance (ASD) to evaluate segmentation conformance. Jacobian determinant to evaluate the quality of the generated DVF.

Experimental setup

- **Experiment design:** ED (moving) to ES (fixed) registration.
- **Preprocessing:** Each slice is cropped to 96×96 with respect to the myocardium centroid after normalization.
- **Implementation:** 1) bspline [6] is implemented using SimpleElastix; 2) optical flow [4] is implemented using scikit-image registration package; 3) learning-based registration is implemented using Pytorch with Adam optimizer with 100 epochs. The learning-based models run 18-30 minutes on a single NVIDIA GTX 2080Ti GPU with 12 GB memory for training and validation.
- **Hyperparameter:** $\nu_p = 0.4$ (Poisson ratio), $\lambda = 0.05$ (weight for BIM loss \mathcal{L}_{reg}), and $\gamma = 0.01$ (weight for auxiliary segmentation loss \mathcal{L}_{seg}).
- **Metrics:** Dice coefficient (DC), Jaccard index (JD), Hausdorff distance (HD), and average symmetric surface distance (ASD) to evaluate segmentation conformance. Jacobian determinant to evaluate the quality of the generated DVF.

Experimental setup

- **Experiment design:** ED (moving) to ES (fixed) registration.
- **Preprocessing:** Each slice is cropped to 96×96 with respect to the myocardium centroid after normalization.
- **Implementation:** 1) bspline [6] is implemented using SimpleElastix; 2) optical flow [4] is implemented using scikit-image registration package; 3) learning-based registration is implemented using Pytorch with Adam optimizer with 100 epochs. The learning-based models run 18-30 minutes on a single NVIDIA GTX 2080Ti GPU with 12 GB memory for training and validation.
- **Hyperparameter:** $\nu_p = 0.4$ (Poisson ratio), $\lambda = 0.05$ (weight for BIM loss \mathcal{L}_{reg}), and $\gamma = 0.01$ (weight for auxiliary segmentation loss \mathcal{L}_{seg}).
- **Metrics:** Dice coefficient (DC), Jaccard index (JD), Hausdorff distance (HD), and average symmetric surface distance (ASD) to evaluate segmentation conformance. Jacobian determinant to evaluate the quality of the generated DVF.

Results

ACDC dataset [1]

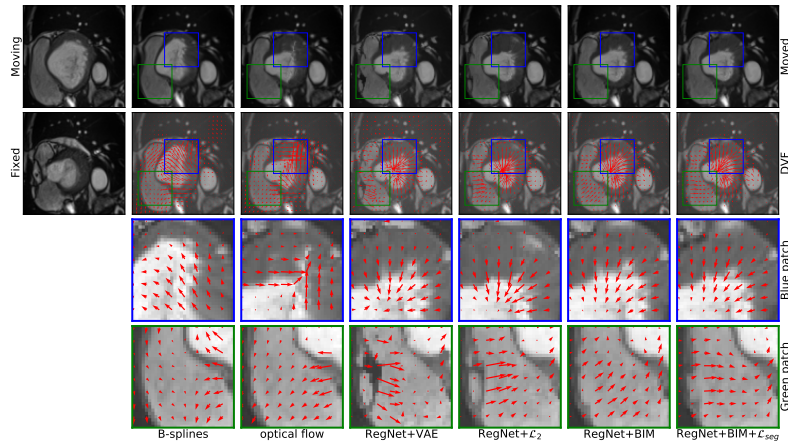


Figure: Visual assessment of registration performance on the ACDC 2017 dataset [1].

Results

ACDC dataset [1]

	Method	Dice[%]↑	Jaccard[%]↑	HD[mm]↓	ASD[mm]↓
LV	affine only	72.01	57.24	11.77	2.13
	B-splines [6]	89.96	82.62	5.37	0.48
	optical flow [4]	87.07	77.87	7.65	0.74
	RegNet+VAE [5]	89.61	81.65	6.46	0.49
	RegNet+ \mathcal{L}_2	89.60	81.68	8.00	0.54
	RegNet+BIM (ours)	90.32	82.70	5.51	0.37
	RegNet+BIM+\mathcal{L}_{seg} (ours)	92.77	86.76	4.39	0.19
RV	affine only	81.08	70.06	14.31	2.21
	B-splines [6]	83.59	74.33	13.70	2.43
	optical flow [4]	84.96	75.94	13.70	2.15
	RegNet+VAE [5]	84.65	75.58	16.48	2.31
	RegNet+ \mathcal{L}_2	84.80	75.73	14.75	2.25
	RegNet+BIM (ours)	85.07	76.16	14.55	2.22
	RegNet+BIM+\mathcal{L}_{seg} (ours)	85.93	77.54	14.07	2.15
Epi	affine only	85.07	74.50	8.61	0.93
	B-splines [6]	92.33	86.12	5.97	0.33
	optical flow [4]	92.02	85.64	6.09	0.39
	RegNet+VAE [5]	91.45	84.83	7.57	0.48
	RegNet+ \mathcal{L}_2	89.92	82.22	7.77	0.59
	RegNet+BIM (ours)	91.53	84.75	6.20	0.40
	RegNet+BIM+\mathcal{L}_{seg} (ours)	92.57	86.48	5.54	0.32

Table: Quantitative assessment of registration performance on the ACDC dataset [1].

Results

ACDC dataset [1]

Method	$ \det(J(\hat{u})) - 1) $
B-splines [6]	0.2489 ± 0.2735
optical flow [4]	0.1283 ± 0.3432
RegNet+VAE [5]	0.0088 ± 0.0100
RegNet+ \mathcal{L}_2	0.0038 ± 0.0051
RegNet+BIM (ours)	0.0035 ± 0.0036
RegNet+BIM+ \mathcal{L}_{seg} (ours)	0.0037 ± 0.0038

Table: Mean Jacobian determinant comparisons on the ACDC 2017 dataset [1].

Conclusions

- We propose a novel data-driven approach for cardiac motion tracking with biomechanics-informed modeling regularization loss.
- Our proposed method generates more realistic DVF in both experiments compared to other competing regularization schemes in visual assessment.
- Our proposed methods outperforms other regularization methods on ACDC 2017 dataset [1] and LV quantification dataset 2019 [7] using quantitative assessment.
- Future work will validate current work on other modalities such as tagged MRI and show its effectiveness in more standardized 3D clinical datasets with additional metrics to assess local abnormalities.

Conclusions

- We propose a novel data-driven approach for cardiac motion tracking with biomechanics-informed modeling regularization loss.
- Our proposed method generates more realistic DVF in both experiments compared to other competing regularization schemes in visual assessment.
- Our proposed methods outperforms other regularization methods on ACDC 2017 dataset [1] and LV quantification dataset 2019 [7] using quantitative assessment.
- Future work will validate current work on other modalities such as tagged MRI and show its effectiveness in more standardized 3D clinical datasets with additional metrics to assess local abnormalities.

Conclusions

- We propose a novel data-driven approach for cardiac motion tracking with biomechanics-informed modeling regularization loss.
- Our proposed method generates more realistic DVF in both experiments compared to other competing regularization schemes in visual assessment.
- Our proposed methods outperforms other regularization methods on ACDC 2017 dataset [1] and LV quantification dataset 2019 [7] using quantitative assessment.
- Future work will validate current work on other modalities such as tagged MRI and show its effectiveness in more standardized 3D clinical datasets with additional metrics to assess local abnormalities.

Conclusions

- We propose a novel data-driven approach for cardiac motion tracking with biomechanics-informed modeling regularization loss.
- Our proposed method generates more realistic DVF in both experiments compared to other competing regularization schemes in visual assessment.
- Our proposed methods outperforms other regularization methods on ACDC 2017 dataset [1] and LV quantification dataset 2019 [7] using quantitative assessment.
- Future work will validate current work on other modalities such as tagged MRI and show its effectiveness in more standardized 3D clinical datasets with additional metrics to assess local abnormalities.

References I

- [1] Olivier Bernard, Alain Lalande, Clement Zotti, Frederick Cervenansky, Xin Yang, Pheng-Ann Heng, Irem Cetin, Karim Lekadir, Oscar Camara, Miguel Angel Gonzalez Ballester, et al. Deep learning techniques for automatic mri cardiac multi-structures segmentation and diagnosis: Is the problem solved? *IEEE transactions on medical imaging*, 37(11):2514–2525, 2018.
- [2] Allen Lu, Shawn S Ahn, Kevinminh Ta, Nripesh Parajuli, John C Stendahl, Zhao Liu, Nabil E Boutagy, Geng-Shi Jeng, Lawrence H Staib, Matthew O'Donnell, et al. Learning-based regularization for cardiac strain analysis via domain adaptation. *IEEE transactions on medical imaging*, 40(9):2233–2245, 2021.
- [3] Xenophon Papademetris, Albert J Sinusas, Donald P Dione, R Todd Constable, and James S Duncan. Estimation of 3-d left ventricular deformation from medical images using biomechanical models. *IEEE transactions on medical imaging*, 21(7):786–800, 2002.

References II

- [4] Javier Sánchez Pérez, Enric Meinhardt-Llopis, and Gabriele Facciolo. Tv-l1 optical flow estimation. *Image Processing On Line*, 2013: 137–150, 2013.
- [5] Chen Qin, Shuo Wang, Chen Chen, Huaqi Qiu, Wenjia Bai, and Daniel Rueckert. Biomechanics-informed neural networks for myocardial motion tracking in mri. In *International Conference on Medical Image Computing and Computer-Assisted Intervention*, pages 296–306. Springer, 2020.
- [6] Daniel Rueckert, Luke I Sonoda, Carmel Hayes, Derek LG Hill, Martin O Leach, and David J Hawkes. Nonrigid registration using free-form deformations: application to breast mr images. *IEEE transactions on medical imaging*, 18(8):712–721, 1999.
- [7] Wufeng Xue, Gary Brahm, Sachin Pandey, Stephanie Leung, and Shuo Li. Full left ventricle quantification via deep multitask relationships learning. *Medical image analysis*, 43:54–65, 2018.

Q & A